Tellus SERIES B CHEMICAL AND PHYSICAL METEOROLOGY
PUBLISHED BY THE INTERNATIONAL METEOROLOGICAL INSTITUTE IN STOCKHOLM

Extreme ozone loss over the Northern Hemisphere high latitudes in the early 2011

By JANUSZ W. KRZYŚCIN*, *Institute of Geophysics, Polish Academy of Sciences, 01-452 Warsaw, Poland*

(Manuscript received 25 August 2011; in final form 31 January 2012)

ABSTRACT

The satellite ozone data comprising The New Zealand National Institute of Water and Atmospheric Research (NIWA) total ozone database version 2.7, total ozone by the Ozone Monitoring Instrument (OMI) spectrophotometer on the Aura platform, and the ozone mixing ratios by SBUV/2 measurements on The National Oceanic and Atmospheric Administration (NOAA) platforms are analysed for ozone variability over the sunlit part of the Northern Hemisphere polar region. An extended area, with unusually low ozone values, is observed in a two-month period beginning in mid February 2011. The total area with extremely depleted total ozone reached the maximum at the end of March 2011, equal to $\sim 11 \times 10^6$ km^2. The area is even larger in the lower/mid stratosphere. A multiple regression model is proposed to attribute the polar total ozone variability to various chemical and dynamical ozone forcings. The model reproduces the ozone loss in early 2011 and the overall picture of the ozone long-term changes. The extreme ozone decline in 2011 could be attributed to the long-lasting period with low stratospheric temperature (<195 K), weaker than the normal Brewer-Dobson circulation, and the Arctic Oscillation in a strong positive phase. A deficit of total ozone in the following summer months (June–July–August), after the total ozone decline in March, was predicted and supported by later OMI observations.

Keywords: polar ozone, satellite observations, multiple regression, dynamical-chemical proxies

1. Introduction

The discovery of the Antarctic ozone hole in the mid-1980s (Chubachi, 1984; Farman et al., 1985) alarmed the scientific community and the public. This discovery indicated that anthropogenic changes were occurring in the ozone layer, shielding the Earth from the harmful solar Ultraviolet (UV) radiation. As the result of this threat, the treaty, called the Montreal Protocol, was signed in 1987 to limit production of ozone-depleting substances (ODS) – man-made chemicals mostly containing chlorine (e.g. freons) and bromine atoms (e.g. halons). Ozone is especially vulnerable to destruction by man-made halogens in the stratosphere, where the strong UV radiation breaks up the ODS molecules, releasing chlorine (or bromine) atoms. One chlorine atom can degrade over 100 000 ozone molecules before it is removed finally from the stratosphere. Bromine is about 60 times more effective in destruction of ozone than chlorine (Yung et al., 1980; WMO, 2010).

Ozone losses intensify over the polar regions when temperature drops below 195 K and polar stratospheric clouds (PSCs) form. Heterogeneous reactions on PSC surfaces convert the chlorine reservoir species to reactive chlorine (Solomon et al., 1986), which can then catalytically destroy ozone, especially over the sunlit areas. The stratosphere in the Southern Hemisphere (SH) over the polar region is colder than that over the Northern Hemisphere (NH), especially in winter (WMO, 2010). Consequently, PSCs are more frequent over Antarctica, causing a stronger ozone destruction over a large area in late winter/spring. The total ozone amount is found to be lower than 220 DU (1 DU $= 2.69 \times 10^{16}$ molecules cm^{-2}) inside the Antarctic polar vortex, the value commonly used as the threshold for the appearance of the so-called Antarctic ozone hole. Since the beginning of the 1980s, the ozone hole over Antarctica appears every year in late August/early September and fills in by December.

The stratospheric chlorine burden over the polar region reached the maximum value in late 1990s and early 2000 and has begun to slightly decrease since then (Newman et al., 2007a; WMO, 2010). During the period of the ODS increase,

*Corresponding author.
email: jkrzys@igf.edu.pl

Citation: Tellus B 2012, **64**, 17347, DOI: 10.3402/tellusb.v64i0.17347

the springtime SH polar ozone values exhibited a declining tendency. A stabilisation of the ozone layer occurred later with trendless year-to-year variations of various characteristics of the ozone hole (such as area, mass deficit and ozone minimum, Newman et al., 2007b). Ozone could not be lowered further because it has been practically removed from the lower stratospheric region of the hole (Douglass et al., 2011). For the Arctic, it was found that only for the coldest Arctic winters, the volume of air cold enough for PSC formation has increased significantly since the late 1960s (Rex et al. 2004; Douglass et al., 2011). The Arctic-spring ozone in the last decade was reported to be lower than that in the 1980s, and also proved to be highly variable from year to year, depending on the strength of the Arctic polar vortex (e.g., Tilmes et al., 2004; Müller et al., 2008; Douglass et al., 2011). The chemical ozone destruction over Arctic in the early 2011 was, for the first time, comparable to that over the Antarctic ozone hole due to unusually long-lasting period, with temperature below the threshold for the potential existence of PSCs (Manney et al., 2011).

This article discusses changes in the area with the extremely low total ozone content in late winter/early spring over the NH high latitudes (poleward of 60°N) since 1979, focusing on the ozone behaviour in 2011. The time series of the area-weighted, high-latitudinal total ozone in late winter/early spring is analysed for an attribution of the ozone trend and its variability in early 2011 to various chemical and dynamical drivers. A prediction of the summer mean of the polar total ozone, which is based on its preceding value in March, is also examined.

2. Data

2.1. Ozone data

The data used here is the version 2.7 of the NIWA combined total column ozone over the sunlit area of the globe, obtained from various satellite measurements for the period 1 January 1979–3 April 2011. NIWA database over 1° (latitude) × 1.25° (longitude) grid comprises the satellite-based ozone measurements from four Total Ozone Mapping Spectrophotometer (TOMS) instruments, three different retrievals from Global Ozone Monitoring Experiment (GOME) and data from four Solar Backscatter Ultraviolet (SBUV) instruments. The data homogenisation and validation procedures were described in Bodeker et al. (2005). No temporal or spatial interpolation was performed on these data.

The database was widely used in various studies of global ozone behaviour (e.g., Newman et al., 2007b; Müller et al., 2008; Douglass et al., 2011). Bias and standard deviation of the differences between the ground-based and the corresponding NIWA total ozone data were found equal to ∼1% and ∼3%, respectively, in the NH mid- and high latitudes (Bodeker et al., 2005).

The NIWA data are extended to the end of August 2011 using the daily total column ozone data obtained from the Ozone Monitoring Instrument (OMI) measurements onboard the NASA's Aura platform. The bias between OMI overpasses and ground-based measurements was less than 1% (McPeters et al., 2008). Therefore, the original OMI data over 1° × 1° grid, available from ftp://toms.gsfc.nasa.gov/pub/omi/data/Level3e/ozone/, are attached to the NIWA data to build the updated ozone database for the period 1 January 1979–31 August 2011. The total ozone data are available for almost all days in the year excluding polar nights.

Figure 1 shows that the ozone data for grid points, located north of 60°N, are available for a region with an area smaller than the corresponding sunlit area. The difference between the database area and the sunlit area is especially large in the period November–February.

The long-term monthly averages for the period 1979–2010 are calculated using the daily total ozone values. The total ozone reference values for each calendar day are obtained from a standard linear interpolation between the long-term monthly means that represent the daily references corresponding to the mid-month days, (i.e., the January monthly mean represents the daily reference for 15th January, the February mean represents 14th February, and so on). Further in the text, the threshold of total ozone, which is 30% below the daily reference, is used to identify extremely low ozone cases over the NH high latitudes. The threshold corresponds to that introduced by Bodeker et al. (2005) when discussing the Antarctic ozone hole area. Their other thresholds of $O_3 < 150$ DU, $O_3 < 220$ DU or O_3 less than 50% of the reference value

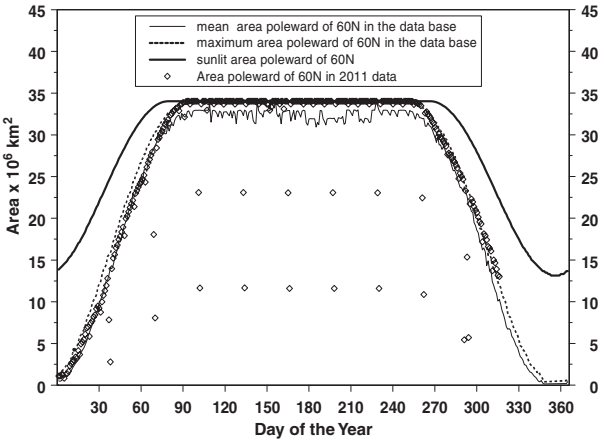

Fig. 1. Seasonal changes of the total sunlit area poleward of 60°N and corresponding area of the region with non-zero total ozone values in the version 2.7 NIWA database.

were not applicable for the Arctic, as such low total ozone values are very rare in this region.

Ozone mixing ratios (OMRs) at selected stratospheric levels (50, 30, 10 and 1 hPa) for the period 2005–2011 are analysed from the daily measurements by the SBUV Radiometer-2 (SBUV/2) onboard the NOAA satellite No. 17. The area weighted daily mean OMRs (ppmv) are calculated over the sunlit latitudes poleward of 60°N using the 3-D daily global ozone database, Stratosphere Monitoring Ozone-Blended Analysis (SMOBA), with the 2.5×2.5 latitude–longitude grid. The output includes OMRs for 24 level ranges, from 0.2 to 1000 hPa. The data are stored as 10-d rotating files at FTP site: ftp.cpc.ncep.noaa.gov/SMOBA/. The ozone profile daily reference values for calculating total area with OMR below the 30% deficit threshold are calculated in the same way as those for the total ozone references. The profile data for 2010 and 2011 are not used for the reference value calculations, because of the extreme behaviour of the NH ozone in 2010 (Steinbrecht et al., 2011; Weber et al., 2011) and in 2011 (Manney et al., 2011).

2.2. *Explanatory variables*

A multiple regression model is proposed for the attribution of the year-to-year variability of high-latitude total ozone to various chemical and dynamical forcings. The following proxies are selected:

- Equivalent effective stratospheric chlorine (EESC) time series parameterising the ozone destruction due to man-made halogens (Fig. 2a), further in the text it is denoted as $EESC(t)$, $t = 1979, \ldots, 2011$.
- Total number of days from 1 December to 15 April of the next year with the minimum temperature in the region being 50–90°N at 50 hPa lower than 195 K (Fig. 2b), that is, temperature allowing the existence

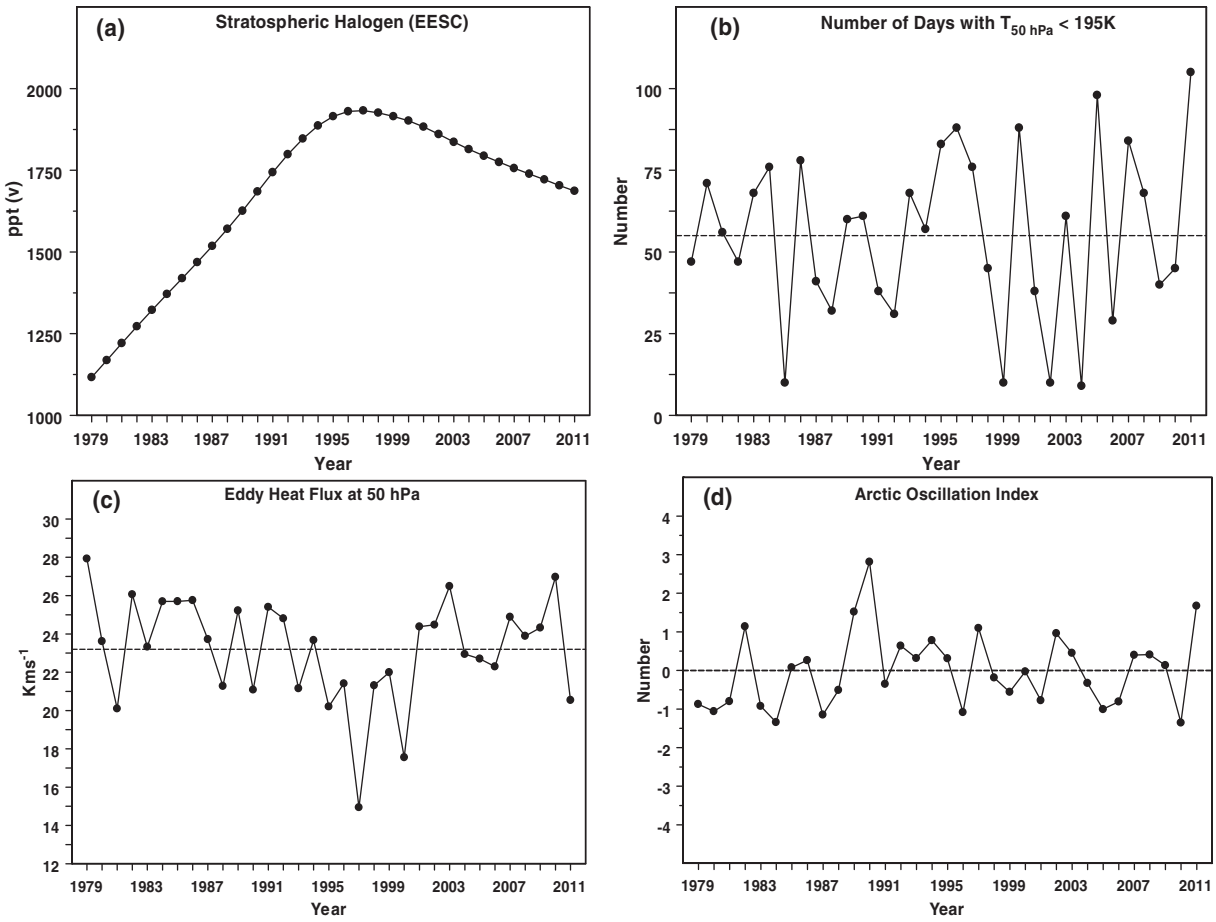

Fig. 2. Proxies used in the statistical modelling of year-to-year total ozone variability: (a) Effective Equivalent Stratospheric Chlorine-EESC, (b) total number of days with the minimum temperature in the 50–90°N region <195 K (the threshold for the potential existence of PSCs), (c) eddy heat flux at 50 hPa averaged over 45–75°N region in the period 1 December–15 April of the next year, (d) the Arctic Oscillation Index. The horizontal lines show the 1979–2011 mean values.

of PSCs. This proxy, denoted as $Proxy_{\mathrm{PSC}}(t)$, is an estimation of the ozone loss due to heterogeneous reactions on the particle surface of the PSCs.

- The mean heat flux at 50 hPa between 45 and 75°N over the period 1 December–15 April of the next year. It is linked to the dynamically driven ozone variability, forced by the Brewer-Dobson circulation (BDC), which redistributes ozone between tropical and polar latitudes (e.g. Weber et al., 2011). This time series (1979–2011), denoted as $Proxy_{\mathrm{BDC}}(t)$, is shown in Fig. 2c.
- The mean Arctic Oscillation (AO) Index for the period February–April. A significant part of the total ozone variability could be attributed to changes of hemispherical atmospheric circulation associated with the AO (e.g. Appenzeller et al., 2000; Thompson et al., 2000). This time series (1979–2011), denoted as $Proxy_{\mathrm{AO}}(t)$, is shown in Fig. 2d.

The $EESC(t)$ time series is according WMO EESC A1_2010A scenario in which fractional releases of the ozone-depleting chemicals are according to Newman et al. (2007a) available from http://acdb-ext.gsfc.nasa.gov/Data_services/automailer. The following parameters are assumed; mean age of air -3.0 yr, width of age of air spectrum -1.5 yr. $EESC(t)$ time series has been frequently used to describe long-term ozone fluctuations (e.g., Newman et al., 2007b; Vyushin et al., 2007; Douglass et al., 2011; Krzyscin, 2012).

Other time series are used for parameterisation of shorter time scale (year-to-year) ozone variations. $Proxy_{\mathrm{PSC}}(t)$, $Proxy_{\mathrm{BDC}}(t)$ are calculated from the annual The National Centers for Environmental Prediction (NCEP) database (http://acdb-ext.gsfc.nasa.gov/Data_services/met/ann_data.html)a. AO index is taken from the NOAA's Climate Prediction Center data: (http://www.cpc.ncep.noaa.gov/products/precip/CWlink/daily_ao_index/ao_index.html).

The overall mean (1979–2011) of $Proxy_{\mathrm{PSC}}(t)$, denoted as $<Proxy_{\mathrm{PSC}}(t)>$, is 54 ± 26 (1σ). The maximum of 104 is found in 2011, which is twice as large as the overall mean value. $Proxy_{\mathrm{BDC}}(2011) = 20.5$ Km s^{-1}, thus it is well below the overall mean, $<Proxy_{\mathrm{BDC}}> = 23.3 \pm 2.73$ Km s^{-1} (1σ). AO index in the early 2011 ($Proxy_{\mathrm{AO}}(2011) = 1.67$) was in its positive phase, $<Proxy_{\mathrm{AO}}> = 0.01 \pm 1.00$ (1σ).

3. Results

3.1. Total ozone deficit area

Figure 3a shows the area poleward of 60°N, with total ozone below the 30% deficit threshold in the period 1 January 2011–31 May 2011. The area used for the total ozone averaging in 2011 was lower than the sunlit area, especially in late autumn and early winter (Fig. 1), but such a discrepancy is typical for the NIWA database. There were only few days in early 2011 with larger area gaps. It seems possible that the area, over which the total ozone was averaged, could vary in previous years as the database comprises the ozone observations collected by different satellite instruments in the period 1979–2011. Thus, for homogenisation of the time series of the total ozone deficit area, we propose the following multiplicative correction factor, $MCF(t)$, to account for the year-to-year variability of the NIWA sampling area for latitudes >60°N:

$$MCF(t) = Area_{\mathrm{MAX}}(t)/Area(t) \quad (1)$$

where $Area(t)$ is the area poleward of 60°N with the total ozone values in the NIWA database for day t, $Area_{\mathrm{MAX}}(t)$ is the corresponding reference value for that day – the maximum area found in the NIWA database in the whole (1979–2011) data period (see Fig. 1). Assuming that the ratio between the ozone deficit area and the whole area with non-zero ozone values will be the same when $Area(t)$ is hypothetically extended to $Area_{\mathrm{MAX}}(t)$, we calculate the corrected size of the 30% total ozone deficit area for day t, $Area\_Cor_{\mathrm{minus30\%}}(t)$, as follows:

$$Area\_Cor_{\mathrm{minus30\%}}(t) = MCF(t) * Area_{\mathrm{minus30\%}}(t) \quad (2)$$

where $Area_{\mathrm{minus30\%}}(t)$ is the actual area in day t with the ozone deficit larger than 30%. The corrected area values are used to draw Fig. 3b, d that correspond to Fig. 3a, c, respectively.

Figure 3a, b show the area poleward of 60°N with total ozone below the 30% deficit threshold in the period 1 January 2011–31 May 2011. Such low ozone values appear almost throughout the whole period since mid-February up to mid-April 2011, with the maximum area of 10.7×10^6 km^2 (Fig. 3a) and 11.03×10^6 km^2 (Fig. 3b) on March 28 that corresponds to about 30% of the high latitude region (latitudes >60°N). Fig. 3c, d illustrate that the maximum size in 2011 was the largest in the period 1979–2011. There is no trend in the yearly time series of the maximum size of 30% deficit area from 15 February–15 April, for the period 1979–2011. However, the statistically significant positive trend appears only when years with high deficit areas ($>3.5 \times 10^6$ km^2) are used for linear regression. The remaining subset of the data is trendless for the period 1979–2011. The results are almost identical for the corrected and for the non-corrected total ozone deficit areas, which supports the robustness of this finding.

Figure 4 illustrates that the extreme low ozone values in 2011 are because of the ozone deficit in the middle stratosphere (Fig. 4a, b). The maximum sunlit area over NH high latitudes with the OMR values below the 30% deficit threshold is $\sim 15 \times 10^6$ km^2 at 50 hPa, and 30 hPa, that is, $\sim 40\%$ larger than the corresponding area for total ozone.

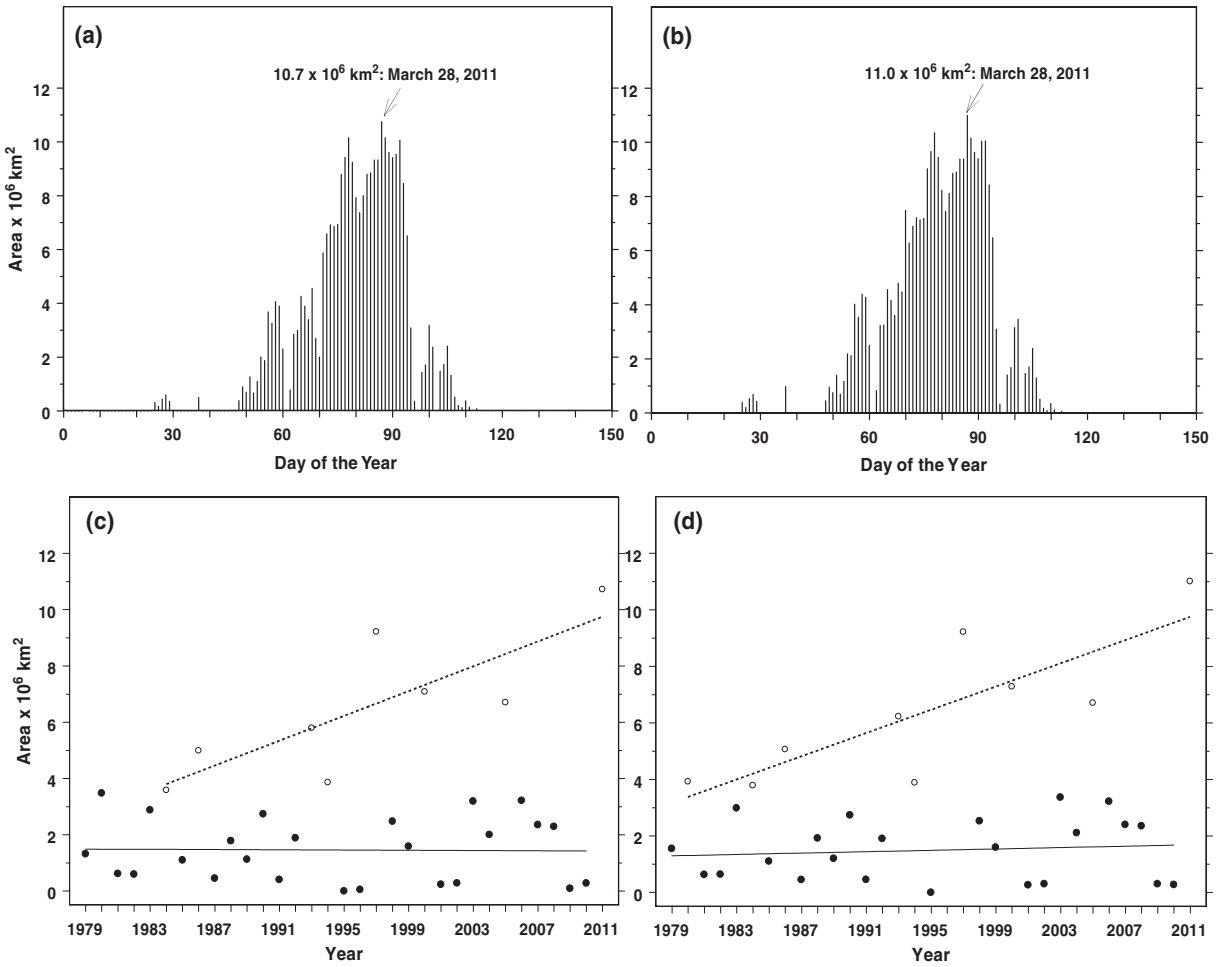

Fig. 3. The area of the polar ($\varphi > 60^\circ$N) region with the total ozone deficit exceeding 30% of the 1979–2010 daily mean values in the period 1 January 2011–31 May 2011 from the original (Fig. 3a) and corrected (Fig. 3b) area data. The time series of the yearly maximum of the deficit area in the 1979–2011 period based on original (Fig. 3c) and corrected (Fig. 3d) area data. Straight lines (Fig. 3c, d) show an ordinary least-squares linear fit to the data subset for years with the large maximum deficit area ($> 3.5 \times 10^6$ km^2) and to the remaining data for years with the low maximum of the deficit area.

3.2. *The regression model*

In section 2.2, we selected the proxies of total ozone to be used in a regression model. The proxies correspond to well known sources (halogen and PSC chemistry, atmospheric dynamics) of ozone variability over the NH high latitudes. A standard least-squares multiple linear fit to the ozone data yields the following regression formula:

$$\begin{aligned} O_3(t) \;=\; & 379.88 \;-\; 0.0406 \cdot (EESC(t) \\ & - EESC(1979)) \;-\; 0.4139 \cdot Proxy_{\mathrm{PSC}}(t) \\ & +\; 3.1454 \cdot Proxy_{\mathrm{BDC}}(t) \;-\; 6.1838 \cdot Proxy_{\mathrm{AO}}(t) \end{aligned} \tag{3}$$

where $t = 1979, \ldots, 2011$, $O_3(t)$ is the area weighted average of total ozone values in the extended NIWA database over sunlit latitudes poleward of 60°N for the period 15 February–15 April in t year. All the regression constants are statistically significant at the confidence level $> 95\%$.

The regression model reproduces the polar ozone variability in the period 1979–2011. R^2, the percent of the explained variance of the analysed ozone series, equals $\sim 74\%$. The model performance is shown in Fig. 5. The year-to-year variations are reproduced by the model. The outliers from the diagonal 1–1 line (Fig. 5a) are the highest in 1992 and 1993, that is, in the period when the polar ozone could be affected by volcanic aerosols after the Pinatubo eruption in June 1991.

The high concentration of the stratospheric aerosols resulted in the additional chemical loss of ~ 35 DU and ~ 55 DU inside the entire polar vortex in late winter/early spring of 1992 and 1993, respectively (Tilmes et al., 2008). Our model supports the known effect of the significant

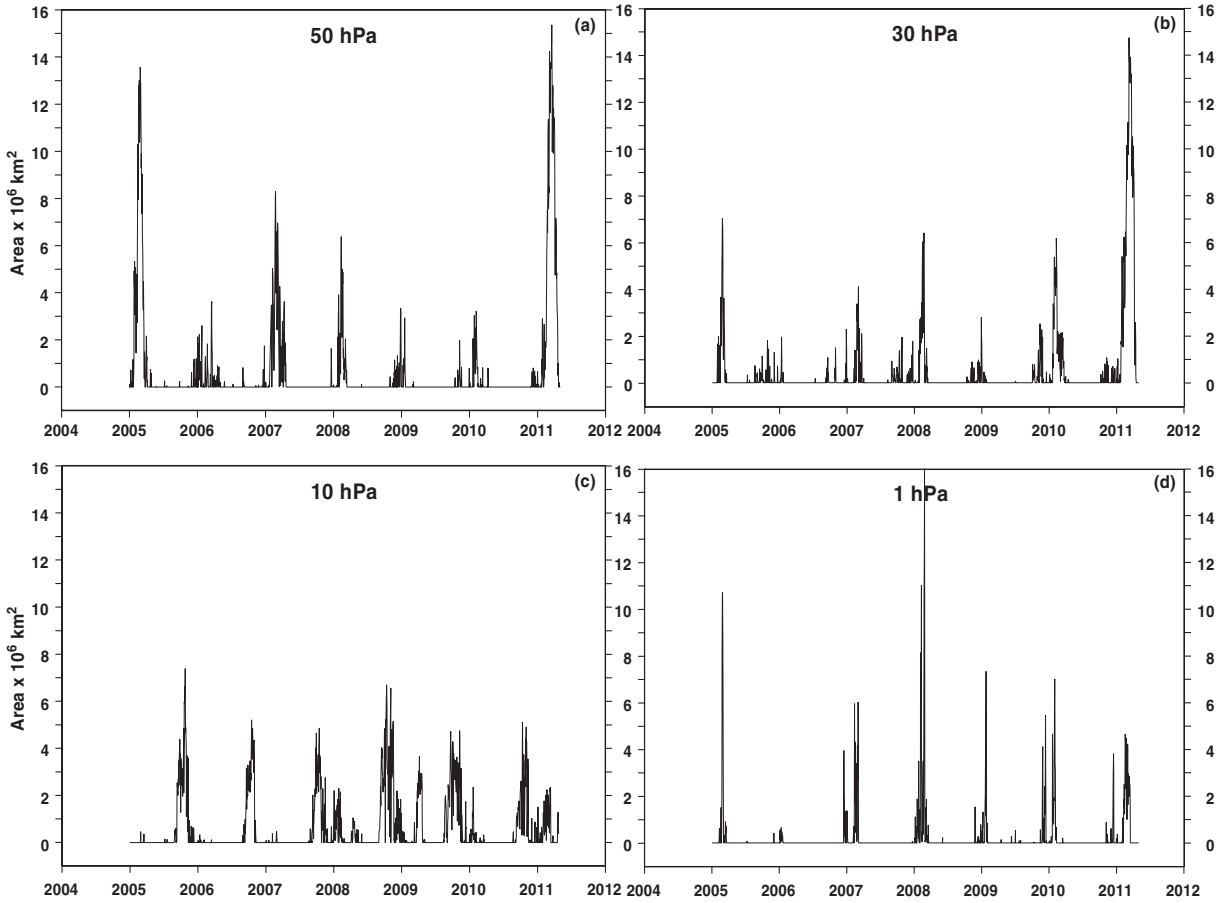

Fig. 4. Size of the polar ($\varphi > 60^{\circ}$N) region with extremely low ozone mixing ratios, i.e., with the deficit larger than 30% of the long-term mean, from measurements by the Solar Backscatter Ultraviolet Radiometer-2 (SBUV/2) onboard of the NOAA satellites in the period 2005–2011 at various levels: (a) 50 hPa, (b) 30 hPa, (c) 10 hPa, and (d) 1 hPa.

polar ozone loss, following strong volcanic eruptions (Rex et al., 2004; Tilmes et al., 2004). However, lower values of the additional ozone loss, that is, $\sim$25 DU and 30 DU in 1992 and 1993, respectively, are estimated as the distance of the outliers in 1992 and 1993 below the one-to-one line in Fig. 5a. The quantitative comparison with the previous results is not possible because our calculations are for the sunlit latitudes poleward of 60°N.

The extreme value of $Proxy_{\mathrm{PSC}}$ in 2011 implies intensive ozone destruction due to heterogeneous reactions on the particle surface of the PSCs in late winter/early spring of 2011. The extra reduction of polar total ozone due to the PSC effect in the period 15 February 2011–15 April 2011, relative to the mean polar ozone destruction (for the period 1979–2011), could be estimated using the output of Model (3), that is, $-0.4139 \cdot (Proxy_{\mathrm{PSC}}(t = 2011) - \langle Proxy_{\mathrm{PSC}} \rangle) \sim -20.7$ DU. The weaker than normal BDC could lead to an additional ozone depletion of $3.1454 \cdot (Proxy_{\mathrm{BDC}}(t = 2011) - \langle Proxy_{\mathrm{BDC}} \rangle) \sim -8.8$ DU. Further, the ozone reduction of 10.4 DU is attributed to the AO positive phase, $Proxy_{\mathrm{AO}}(t = 2011) = 1.675$. The observed ozone in early 2011 is the third smallest value in the whole 1979–2011 time series, that is, lower by about 12% than the long-term mean value (410 DU) for the period 1979–2010.

The model reproduces the overall pattern of the long-term variability of the high latitudinal total ozone in late winter/early spring, with decreasing tendency up to the mid-1990s, which is replaced by a slight increase afterwards (Fig. 5b). The modelled long-term trend underestimates only slightly the observed one in the 2000s.

Figure 6 shows that the polar ozone deficit appearing in March implies low total O_3 in the following summer. The positive correlation between late winter/early spring total ozone and corresponding subsequent summer values over the polar NH has been previously discussed by Krzyscin et al. (2001), Fioletov and Shepherd (2003) and Weber et al. (2011). There are no mechanisms for significant changes in the high latitudinal ozone after the end of the ozone build-up period (spring) because of the disappearance of the

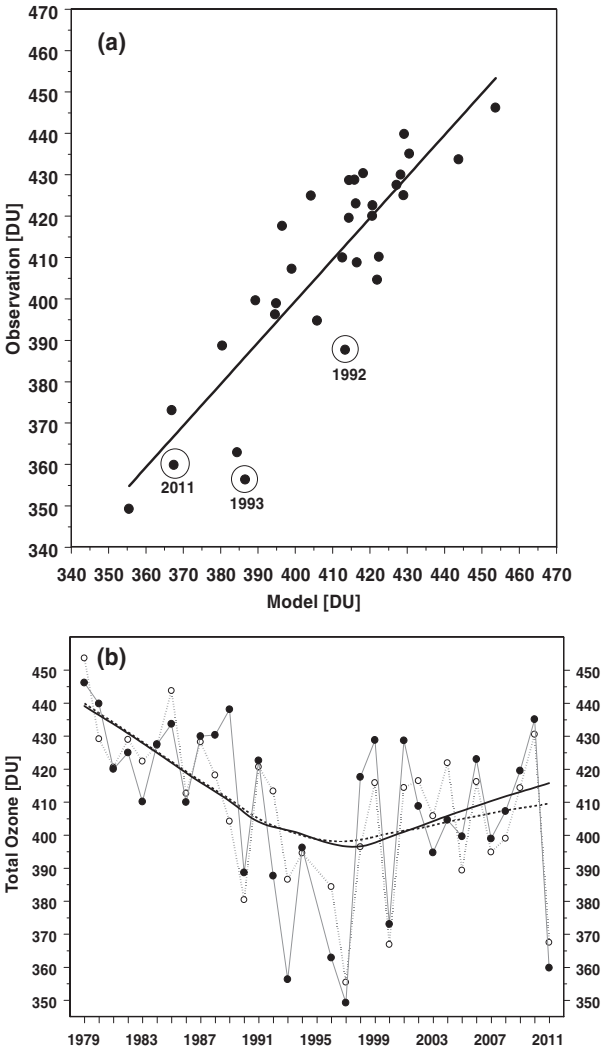

Fig. 5. Performance of the statistical model: (a) observed (version 7.2 NIWA total ozone) versus modelled values of the area-weighted total ozone averaged over the period 15 February–15 April, (b) corresponding time series (1979–2011) of the observed (full circles and solid curve) and modelled (open circles and dashed curve) late winter/early spring total ozone values. The curves represent the data smoothed by the LOWES regression.

PSCs and a weakening of BDC in NH in later months. Taking into account the regression line shown in Fig. 6, the mean polar ozone of $\sim$312 DU could be anticipated in the summer (June–July–August) of 2011. The record low summer mean ozone value of $\sim$309 DU is found in 2011, that is, close to the predicted value from the regression line shown in Fig. 6. The summer mean in 1993 was even lower ($\sim$295 DU), but there were many missing days in June and early July in that year. Moreover, total ozone in 1993 was also influenced by Pinatubo. The summer mean of total polar ozone in 2011 is $\sim$3.6% lower than the overall

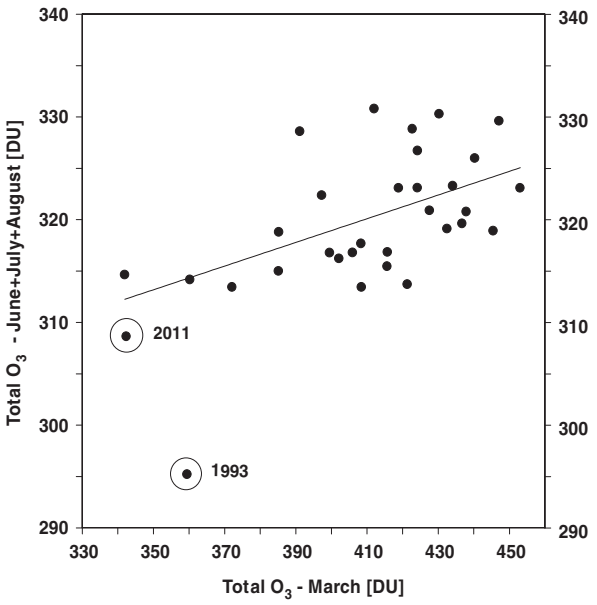

Fig. 6. Summer means (1 June–31 August) of the area weighted polar ($\varphi > 60°$N) total ozone versus the preceding March total ozone mean.

summer mean for the period 1979–2010. Such a change in total ozone would increase the erythemally weighted solar irradiance of $\sim$4% in cloud-free days in the summer of 2011, that is, in the period of naturally high solar UV irradiation at the Earth's surface.

4. Summary and conclusions

We focus on the ozone data over the polar sunlit latitudes to reveal a potentially excessive solar UV radiation due to low ozone in this region. Massive ozone destruction occurred also inside the polar vortex ozone, especially in early 2011 (Manney et al., 2011), in a dark region, but it had no immediate impact on the solar UV radiation there. In March and April 2011, substantially elevated UV indices were found for some Arctic and sub-Arctic sites (Bernhard et al., 2011).

In late March 2011, the area poleward of 60°N, with the extremely low daily total ozone, that is, below 30% of the overall long-term daily mean, reaches the maximum value of $\sim 11 \times 10^6$ km^2 over the whole period (1979–2011) of the total ozone observations by satellite spectrophotometers. Almost continuously for two months (mid-February up to mid-April 2011), highly depleted total ozone values are found poleward of 60°N. The total area, with the ozone mixing ratio deficit greater than 30% mean, appears to be even larger, $\sim 15 \times 10^6$ km^2, at the 50 hPa and 30 hPa levels.

The yearly means of the area-weighted polar total ozone in late winter/early spring (15 February–15 April) are calculated for the period 1979–2011 by averaging the daily total ozone values for latitudes $>60^{\circ}$N. The ozone data are taken from the NIWA database comprising the satellite measurements over the polar sunlit area. Thus, the UV overexposure threat over the polar region could be estimated based on the NIWA polar total ozone data.

The late winter/early spring polar ozone in 2011, which is smaller than the overall long-term (1979–2010) mean by $\sim$12%, appears to be the third smallest mean for the whole period (1979–2011). The average total ozone value in March 2011 sets a new record-low value, 342 DU, for all Marches in the period 1979–2011. Moreover, the summer mean in 2011 based on daily ozone values in the period June–July–August of 309 DU is the smallest in the whole record of the summer means in the period 1979–2011, if the total ozone mean for summer 1993 is excluded from the record because of limited number of satellite observations in that season.

We propose the regression model to attribute the polar-ozone variability in late winter/early spring to various chemical and dynamical ozone forcings. The model accounts for the ozone chemical destruction by man-made halogens and heterogeneous reactions on the particle surface of the PSCs, and the dynamical ozone forcing due to year-to-year changes in the hemispherical atmospheric circulation patterns (BDC and AO). The modelled polar ozone in 2011 almost perfectly matches the observed one. The ozone reduction in 2011 is found to be the result of extreme weather conditions allowing more PSCs, weaker BDC and AO in a strong positive phase.

It seems that the ozone loss in the early 2011 is in accordance with the hypothesis of continuation of more severe ozone extremes in the series of 'cold' Arctic winters (Rex et al. 2004; Douglass et al., 2011). The ozone recovery over the Arctic is expected in the next decades because of the reversed trend in the ODS concentration in the stratosphere since the late 1990s, after few decades of intense increase. This reversed trend could be linked with the ODS production limits set by regulations of the Montreal Protocol 1987 and its amendments and adjustments (Mäder et al., 2010; WMO, 2010). Moreover, there is an expectation of intensification of BDC, which is inferred from 3-D chemical-chemistry models (Li et al., 2009; Waugh et al., 2009), causing an enhanced ozone transport to the NH polar latitudes in winter/early spring.

5. Acknowledgements

This work was partially supported by a grant from the State Inspectorate for Environment Protection in Poland, under contract No. 48/2010/F. We are grateful to two anonymous reviewers for helpful comments. We thank G. Bodeker for providing the Bodeker Scientific/NIWA total ozone database.

References

Appenzeller, C., Weiss, A. and Staehelin, J. 2000. North Atlantic Oscillation modulates total ozone winter trends. *Geophys. Res. Lett.* **27**, 1131–1134.

Bernhard, G., Manney, G., Fioletov, V., Grooss, J.-U., Heikkilä, A., and co-authors. 2011. *Ozone and UV Radiation, Arctic Report Card 2011*. Online at: http://www.arctic.noaa.gov/reportcard

Bodeker, G. E., Shiona, H. and Eskes, H. 2005. Indicators of Antarctic ozone depletion. *Atmos. Chem. Phys.* **5**, 2603–2615.

Chubachi, S. 1984. Preliminary result of ozone observations at Syowa station from February 1982 to January 1983. *Mem. Natl. Inst. Polar Res. Spec. Issue Jpn.* **34**, 13–20.

Douglass, A., Fioletov, V., Arola, A., Burkholder, J. B., Burrows, J. P. and co-authors. 2011. Stratospheric ozone and surface ultraviolet radiation. In *Scientific Assessment of Ozone Depletion: 2010* (ed. Christine A. Ennis). chap. 2. Global Ozone Research and Monitoring Project-Report No. 52. World Meteorological Organization, Geneva, Switzerland, 516 pp.

Farman, J. C., Gardiner, B. G. and Shanklin, J. D. 1985. Large losses of total ozone in Antarctica reveal seasonal ClOx/NOx interaction. *Nature*. **315**, 207–210.

Fioletov, V. E. and Shepherd, T. G. 2003. Seasonal persistence of mid latitude total ozone anomalies. *Geophys. Res. Lett.* **30**(7), 1417. DOI: 10.1029/2002GL016739

Krzyscin, J. W. 2012. Onset of the total ozone increase based on statistical analyses of global ground-based data for the period 1964–2008. *Int. J. Climatol.* **32**(2), 240–246.

Krzyscin, J. W., Degórska, M. and Rajewska-Wi(ch, B. 2001. The summer-midwinter correlation in total ozone over North America and Europe for the period 1963–1997. *J. Atmos. Sol. Terr. Phys.* **63**, 1499–1507.

Li, F., Stolarski, R. S. and Newman, P. A. 2009. Stratospheric ozone in the post-CFC era. *Atmos. Chem. Phys.* **9**, 2207–2213. DOI: 10.5194/acp-9-2207-2009

Mäder, J. A., Staehelin, J., Peter, T., Brunner, D., Rieder H. E. and co-authors. 2010. Evidence for the effectiveness of the Montreal Protocol to protect the ozone layer. *Atmos. Chem. Phys.* **10**, 12161–12171.

Manney, G. L., Santee, M. L., Rex, M., Livesey, N. J., Pitts, M. C. and co-authors. 2011. Unprecedented Arctic ozone loss in 2011. *Nature*. **478**, 469–475. DOI: 10.1038/nature10556

McPeters, R., Kroon, M., Labow, G., Brinksma, E., Balis, D. and co-authors. 2008. Validation of the Aura Ozone Monitoring Instrument total column ozone product. *J. Geophys. Res.* **113**, D15S14. DOI: 10.1029/2007JD008802

Müller, R., Grooss, J.-U., Lemmen, C., Heinze, D., Dameris, M. and co-authors. 2008. Simple measures, of ozone depletion in the polar stratosphere. *Atmos. Chem. Phys.* **8**, 251–264.

Newman, P. A., Daniel, J. S., Waugh, D. W. and Nash, E. R. 2007a. A new formulation of equivalent effective stratospheric chlorine (EESC). *Atmos. Chem. Phys.* **7**, 4537–4552.

Newman, P. A., Rex, M., Canziani, P. O., Carslaw, K. S., Drdla, K. and co-authors. 2007b. Polar Ozone: past and present. In: *Scientific Assessment of Ozone Depletion: 2006* (ed. Christine A. Ennis). chap. 4. Global Ozone Research and Monitoring Project-Report No. 50. World Meteorological Organization, Geneva, Switzerland, 572 pp.

Rex, M. J., Salawitch, R. J., von der Gathen, P., Harris, N. R. P., Chiperfield, M. P. and co-author. 2004. Arctic ozone loss and climate change. *Geophys. Res. Lett*. **31**, L04116. DOI: 10.1029/2003GL018844

Solomon, S., Garcia, R. R., Rowland, F. S. and Wuebbles, D. J. 1986. On the depletion of Antarctic ozone. *Nature*. **321**, 755–758.

Steinbrecht, W., Köhler U, Claude, H., Weber, M., Burrows, J. P. and co-author. 2011. Very high ozone columns at northern mid-latitudes in 2010. *Geophys. Res. Lett*. **38**, L06803. DOI: 10.1029/2010GL046634

Thompson, D. W., Wallace, J. M. and Hegrl, G. C. 2000. Annular mode in the extratropical circulation. Part II: trends. *J. Clim*. **13**, 1018–1036.

Tilmes, S., Müller, R., Grooss, J.-U. and Russell, J. M. 2004. Ozone loss and chlorine activation in the Arctic winters 1991–2003 derived with the tracer-tracer correlations. *Atmos. Chem. Phys*. **4**, 2181–2213.

Tilmes, S., Müller, R. and Salawitch, R. J. 2008. The sensitivity of polar ozone depletion to proposed geoengineering schemes. *Science*. **320**, 1201–1204. DOI: 10.1126/science.1153966

Vyushin, D., Fioletov, V. E. and Shepherd, T. G. 2007. Impact of long-range correlations on trend detection in total ozone. *J. Geophys. Res*. **112**, D14307.1–D14307.18. DOI: 10.1029/2006JD008168

Waugh, D. W., Oman, L., Kawa, S. R., Stolarski, R. S., Pawson, S. and co-authors. 2009. Impacts of climate change on stratospheric ozone recovery. *Geophys. Res. Lett*. **36**, L03805. DOI: 10.1029/2008GL036223

Weber, M., Dikty, S., Burrows J. P., Garny H., Dameris, M. and co-authors. 2011. The Brewer-Dobson circulation and total ozone from seasonal to decadal time scales. *Atmos. Chem. Phys*. **11**, 11221–11235.

World Meteorological Organization (WMO). 2010. Scientific assessment of ozone depletion: 2010 (ed. Christine A. Ennis). Global Ozone Research and Monitoring Project. Report No. 52, Geneva, Switzerland, 516 pp.

Yung, Y. L., Pinto, J. P., Watson, R. T. and Sander, S. P. 1980. Atmospheric bromine and ozone perturbations in the lower stratosphere. *J. Atmos. Sci*. **37**, 339–353.